Inorganic Chemistry

Article

pubs.acs.org/IC

Syntheses, X-ray Structural Characterizations, and Thermal Stabilities of Two Nonclassical Trinuclear Vanadium(IV) Complexes, $(V_3(\mu_3\text{-}O)O_2)(\mu_2\text{-}O_2P(CH_2C_6H_5)_2)_6(H_2O)$ and $(V_3(\mu_3\text{-}O)O_2)(\mu_2\text{-}O_2P(CH_2C_6H_5)_2)_6(py)$, and Polymeric Complexes of Stoichiometry $(VO(O_2PR_2)_2)_\infty$, $R_2 = Ph_2$ and $o\text{-}(CH_2)_2(C_6H_4)$

John S. Maass,[†] Zhichao Chen,[†] Matthias Zeller,[‡] Floriana Tuna,[§] Richard E. P. Winpenny,[§] and Rudy L. Luck*,[†]

[†]Department of Chemistry, Michigan Technological University, 1400 Townsend Drive, Houghton, Michigan 49931, United States

[‡]Department of Chemistry, Youngstown State University, 1 University Plaza, Youngstown, Ohio 44555, United States

[§]School of Chemistry, The University of Manchester, Oxford Road, Manchester, M13 9PL, U.K.

Supporting Information

ABSTRACT: The preparation and structural characterization of two trinuclear vanadium complexes, $(V_3(\mu_3\text{-}O)O_2)(\mu_2\text{-}O_2P(CH_2C_6H_5)_2)_6(H_2O)$, **1**, and $(V_3(\mu_3\text{-}O)O_2)(\mu_2\text{-}O_2P(CH_2C_6H_5)_2)_6(py)$, **2**, are reported. In these nonclassical structures, the planar central core consists of the three vanadium atoms arranged in the form of an acute quasi-isosceles triangle with the central oxygen atom multiply bonded to the vanadium atom at the center of the vertex angle and weakly interacting with the two other vanadium atoms on the base sites, each of which contain one external multiply bonded oxygen atom. Reacting $VO(acac)_2$ in the presence of diphenylphosphinic acid affords $(VO(O_2PPh_2)_2)_\infty$, **3**, while 2-hydroxyisophosphindoline-2-oxide at room temperature in CH_2Cl_2 affords $((H_2O)VO(O_2P\text{-}o\text{-}(CH_2)_2C_6H_4)_2)_\infty$, **4**, and at 120 °C in EtOH yields $(VO(O_2P(o\text{-}(CH_2)_2(C_6H_4))_\infty$, **5** on the basis of elemental analyses. The thermal and chemical stability of the complexes were assessed by thermogravimetric analysis (TGA) and differential scanning calorimetry (DSC) measurements. The bond strengths of the vanadium atoms to the OH_2 ligand in **1** and to the NC_5H_5 ligand in **2** were assessed at 10.7 and 42.0 kJ/mol respectively. Room temperature magnetic susceptibility measurements reveal magnetic moments for trinuclear **1** and **2** at 3.02(1) and 3.05(1) $\mu_{B/mol}$, and also close to spin only values (1.73 μ_B) values for **3**, **4**, and **5** at 1.77(2), 1.758(7), and 1.77(3) μ_B, respectively. Variable-temperature, solid-state magnetic susceptibility measurements were conducted on complex **2** in the temperature range of 2.0−298 K and at an applied field of 0.5 T. Magnetization measurements at 2 and 4 K confirmed a very weak magnetic interaction between the vanadyl centers.

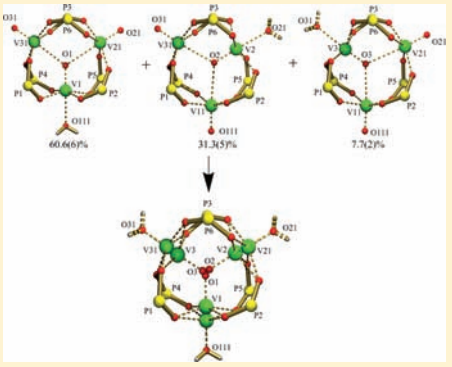

1. INTRODUCTION

We have previously detailed the formation of tetrameric clusters of molybdenum(V) stabilized by phosphinate ligands and described their capabilities as catalysts for the epoxidation of olefins.[1−3] More recently, we communicated the syntheses and single crystal structures of vanadium(V) and tungsten(V) tetrameric clusters.[4] Vanadium is worthy of exploration as it is a catalyst for the industrial production of maleic anhydride,[5] it is the active metal central in some halogenating enzymes of marine organisms,[6] some vanadium compounds have been found to be effective in treating diabetes,[7] and more relevant, there is a very large quantity of oxovanadium compounds stabilized by phosphonic acids[8] but not many containing phosphinate ligands.[9−12] In that regard, the diphenylphosphinate ligand was previously utilized as a model for the interaction of phosphate ligands with oxo-bridged di-Fe proteins[13,14] and in reactions with Co which resulted in polymers.[15] We were most interested in studying how oxidovanadium(IV), VO^{2+}, would coordinate with different phosphinate ligands.

To the best of our knowledge, the only compounds reported that contain phosphinate ligands coordinated to oxidovanadium(IV) characterized by crystallography are dimeric compounds of the general formula $[(VO)_2(\mu\text{-}L)_2(HB(pz)_3)_2]$ (L = diphenylphosphinate or monophenylphosphinate)[9] and $[(VO)_2(\mu\text{-}L_1)_3(L_2)_2]NO_3$ (L_1 = diphenylphosphinate or bis(4-methoxyphenyl)phosphinate, L_2 = 2,2′-bipyridine[10] or 1,10-phenanthroline)[11] and the 2D-layered diphosphinate, $[VO(O_2\text{-}(C_6H_5)PCH_2P(C_6H_5)O_2)]$.[12] Interestingly, trinuclear vanadium clusters have been reported stabilized by carboxylate groups. For example, five compounds of the trinuclear formulation $[V_3O\text{-}(RCO_2)_6L_3]^{0,+}$, two with valencies II, III, III, and three with III, III, III,

Received: June 11, 2011
Published: February 16, 2012

   dx.doi.org/10.1021/ic201259u | Inorg. Chem. 2012, 51, 2766−2776

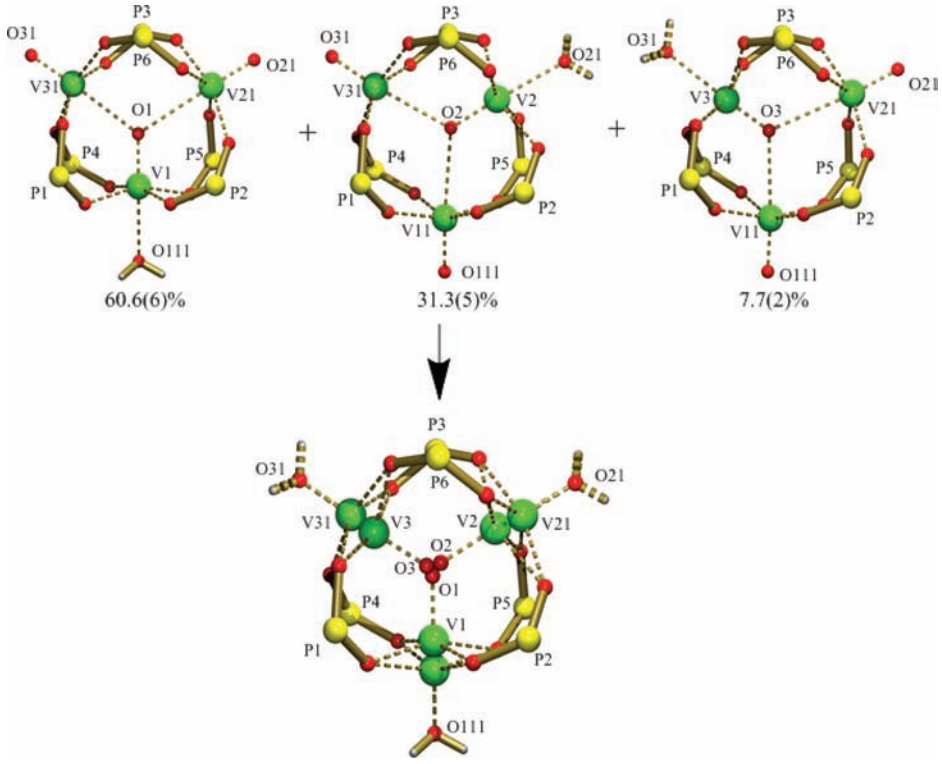

Figure 1. POV-Ray rendered Platon[27] constructed representations of the nature of the disorder in **1**. For clarity the dibenzylphosphinate ligands are represented by "PO_2" fragments.

were reported as containing a central oxo ligand in the center of an equilateral "V_3" triangle of D_{3h} symmetry referred to as classical.[16,17] A less symmetrical example (i.e., containing an almost centrally located oxo ligand but one V···V distance at 3.068(2) Å is shorter than the other two at 3.43(2) and 3.349(2) Å) of this type of trinuclear cluster is $[Et_3NH][V^{III}_3(\mu_3\text{-}O)(Salox)_2(HSalox)(Salmp)]$, where H_2Salox = salicylaldoxime and H_3Salmp = 2-(bis(salicylideneamino)methyl)phenol.[18] In contrast, the less symmetrical $[V_3(\mu_3\text{-}O)O_2]^{6+}$ core, in which the central oxygen atom is doubly bonded to one vanadium atom, weakly bonded to the other two vanadium atoms and all vanadium atoms exhibited valencies of IV, was earlier reported for the compounds $(V_3(\mu_3\text{-}O)O_2)(\mu_2\text{-}O_2CC_6H_5)_6(THF)$,[19] $[(V_3(\mu_3\text{-}O)O_2)((C_2H_5O)_2PO_2)_6\cdot CH_3CN]$,[5] and $[(V_3(\mu_3\text{-}O)O_2)(BrC(CH_3)COO)_6(HO^iPr)$.[20] Here the three vanadium atoms are in the form of quasi-isosceles triangles displaying C_{2v} symmetry or the nonclassical form. The $[V_3(\mu_3\text{-}O)O_2]^{6+}$ cation was stabilized by the six bridging benzoate or diethylphosphate molecules and either a THF or CH_3CN ligand was bonded trans to the $V{=}O_{center}$ bond. As stated,[5,19] these compounds do not contain true "$M_3(\mu_3\text{-}O)$" cores in which the central oxygen atom in the "$(V_3(\mu_3\text{-}O)O_2)$" moiety is located equidistant from the three metal atoms, but they are a cluster of three oxidovanadium(IV) ions. This difference is due to the fact that the oxygen atoms are more strongly bonded to the more positively charged vanadium(IV) atoms (i.e., as $(V{\equiv}O)_3$).

We report here on the use of dibenzylphosphinate ligands to synthesize the compounds $(V_3(\mu_3\text{-}O)O_2)(\mu_2\text{-}O_2P(CH_2C_6H_5)_2)_6(H_2O)$, **1**, and $(V_3(\mu_3\text{-}O)O_2)(\mu_2\text{-}O_2P(CH_2C_6H_5)_2)_6(py)$, **2**. These both contain asymmetrical centrally located oxo ligands, that is, the nonclassical forms which display C_{2v} symmetry. Reactions between $VO(acac)_2$ and diphenylphosphinic acid resulted an intractable substance analyzing as $(VO(O_2PPh_2)_2)_\infty$, **3**, while reactions with 2-hydroxyisophosphindoline-2-oxide[21] at room temperature in CH_2Cl_2 affords $((H_2O)VO(O_2P(o\text{-}(CH_2)_2(C_6H_4))_\infty$, **4**, and at 120 °C in EtOH yields $(VO(O_2P(o\text{-}(CH_2)_2(C_6H_4))_\infty$, **5**. The crystal structures of **1**, a cocrystallized mixture consisting of 21.7(6)% **1** and 78.3(6)5% **2** and pure **2**, and the thermal gravimetric analysis (TGA), differential scanning calorimetry (DSC), room temperature magnetic susceptibility measurements on **1**−**5** and the variable temperature magnetic susceptibility measurements and low temperature magnetization measurements for complex **2** are described.

2. EXPERIMENTAL SECTION

2.1. General Methods. Chemicals were purchased from Aldrich Chemicals and solvents were used as received. Elemental analyses were conducted by Galbraith Laboratories, Knoxville, TN. IR spectra were recorded on a PerkinElmer Spectrum One spectrometer (neat). The TGA and DSC analyses were conducted on Shimadzu TGA-50 and DSC-50 analyzers and under a slow N_2 (not O_2 exclusive) stream. Magnetic measurements were conducted on a Johnson Matthey Auto MSB instrument. The powder diffraction X-ray data were obtained using a Scintag XDS-2000 θ/θ diffractometer. Dibenzylphosphinic acid and hydroxyisophosphindoline-2-oxide,[21] diphenylphosphinic acid,[22] $VO(acac)_2$,[23] and $VO(acac)_2(py)$[23,24] were prepared according to the cited literature. Their FTIR spectra are presented as Supporting Information Figures S1 and S2 for $VO(acac)_2$ and $VO(acac)_2(py)$, respectively. The variable temperature magnetic susceptibility measurement was performed on a polycrystalline sample of **2** in the temperature range 2.0−298 K and at an applied field of 0.5 T using a Quantum Design MPMS SQUID magnetometer. The sample holder diamagnetism was measured and subtracted from the raw data. Magnetization measurements were performed at 2 and 4 K.

2.2. Synthesis. *2.2.1. Synthesis of $(V_3(\mu_3\text{-}O)O_2)(\mu_2\text{-}O_2P(CH_2C_6H_5)_2)_6(H_2O)$ (1).* $VO(acac)_2$ (0.200 g, 0.754 mmol) and 0.392 g (1.585 mmol) of dibenzylphosphinic acid were placed in a sealed tube with 5 mL of ethanol and heated at 120 °C for 16 h. A light blue precipitate formed, which was isolated by filtration and recrystallized from methylene chloride and hexane

dx.doi.org/10.1021/ic201259u | Inorg. Chem. 2012, 51, 2766−2776

Table 1. Crystal Data and Refinement Details of Crystals A Containing 1, B Containing 2 and 1 in a 78.3(6):21.7(6) Respective Ratio, and Pure 2

	A	B	2
chemical formula sum	$C_{175}H_{186}Cl_{14}O_{32}P_{12}V_6$	$C_{87.91}H_{88.34}N_{0.78}O_{15.22}P_6V_3$	$C_{89}H_{89}NO_{15}P_6V_3$
fw (g)	3974.72	1737.88	1751.25
temperature (K)	100(2)	100(2)	100(2)
wavelength (Å)	0.71069	0.71069	0.71069
cryst syst	monoclinic	triclinic	triclinic
space group	$P2_1/c$	$P1$	$P1$
unit cell dimensions (Å, deg)	a = 26.630(1), α = 90	a = 13.1842(8), α = 108.063(1)	a = 13.248(2), α = 108.30(1)
	b = 20.903(8), β = 90.804(9)	b = 13.7341(9), β = 103.954(1)	b = 13.779(2), β = 103.97(1)
	c = 16.779(7), γ = 90	c = 13.9398(9), γ = 110.953(1)	c = 14.050(1), γ = 110.889(2)
volume (Å^3)	9339(6)	2057.4(2)	2086.7(5)
Z	2	1	1
density (calculated, mg/m^3)	1.413	1.413	1.394
abs coeff (mm^{-1})	0.659	0.517	0.510
F(000)	4096	909	909
cryst size (mm)	0.50 × 0.31 × 0.13	0.36 × 0.36 × 0.08	0.45 × 0.26 × 0.15
θ range for data collection (deg)	0.76−29.59	1.67−31.44	1.66−31.43
index ranges	$-32 \le h \le 36$, $-28 \le k \le 28$, $-21 \le l \le 23$	$-18 \le h \le 18$, $-20 \le k \le 20$, $-19 \le l \le 19$	$-18 \le h \le 19$, $-18 \le k \le 19$, $-20 \le l \le 20$
reflns collected	66641	25292	25844
independent reflns	25531 [R(int) = 0.0640]	21357 [R(int) = 0.0255]	21017 [R(int) = 0.0242]
abs correction	multiscan	multiscan	multiscan
max. and min transmission	0.9192 and 0.7340	0.9598 and 0.8356	0.9274 and 0.8029
data/restraints/params	25531/46/1212	21357/279/1085	21017/3/1027
GOF on F^2	1.028	1.001	0.998
Final R indices [$I > 2\sigma(I)$]	R_1 = 0.0712,[a] R_2 = 0.1822[b,c]	R_1 = 0.0516, R_2 = 0.1112[b,d]	R_1 = 0.0475, R_2 = 0.0990[b,e]
R indices (all data)	R_1 = 0.1268, R_2 = 0.2125	R_1 = 0.0773, R_2 = 0.1196	R_1 = 0.0617, R_2 = 0.1085
max diff. peak and hole (e·Å^{-3})	1.397 and −1.555	1.118 and −0.605	0.916 and −0.492

[a] $R_1 = \sum||F_o| - |Fc||/\sum|F_o|$. [b] $R_2 = [\sum[w(F_o^2 - F_c^2)^2]/\sum[w(F_o^2)^2]]^{1/2}$. [c] $w = 1/[\sigma^2(F_o^2) + (0.0924P)^2 + 15.7040P]$, where $P = (F_o^2 + 2(F_c)^2)/3$. [d] $w = 1/[\sigma^2(F_o^2) + (0.0532P)^2 + 0.0000P]$. [e] $w = 1/[\sigma^2(F_o^2) + (0.0496P)^2 + 0.0000P]$.

resulting in 0.340 g (0.200 mmol, 79.6% yield based on VO(acac)$_2$) of $(V_3(\mu_3\text{-}O)O_2)(\mu_2\text{-}O_2P(CH_2C_6H_5)_2)_6(H_2O)$ (**1**). Anal. Calcd for $C_{84}H_{86}O_{16}P_6V_3$: C, 59.69; H, 5.13. Found: C, 59.52; H, 5.36%. IR (Supporting Information Figure S3, neat, cm^{-1}) 3628 vw, 3537 vw, 3062 vw, 3029 vw, 2909 vw, 1602 w, 1496 m, 1453 m, 1400 w, 1234 w, 1189 m, 1164 m, 1103 m, 1024 vs, 995 sh, 942 m, 915 m, 840 s, 806 s, 732 m, 695 vs.

*2.2.2. Synthesis of $(V_3(\mu_3\text{-}O)O_2)(\mu_2\text{-}O_2P(CH_2C_6H_5)_2)_6(py)$ (**2**).* $(V_3(\mu_3\text{-}O)O_2)(\mu_2\text{-}O_2P(CH_2C_6H_5)_2)_6(py)$, **2**, was produced by mixing 0.050 g (0.186 mmol) of VO(acac)$_2$, 0.093 g (0.376 mmol) of dibenzylphosphinic acid, and 2 drops of pyridine in 5 mL of methylene chloride. The mixture was stirred overnight at room temperature. It was then filtered, concentrated, and the subsequent addition of hexanes resulted in 0.070 g (0.040 mmol, 63.25% based on VO(acac)$_2$) of **2**. Anal. Calc. for $C_{89}H_{91}O_{15}P_6V_3N$: C, 60.75; H, 5.12. Found: C, 60.44; H, 5.40%. IR (Supporting Information Figure S4, neat, cm^{-1}) 3062 vw, 3028 vw, 2911 vw, 1602 w, 1496 m, 1454 m, 1400 w, 1234 m, 1189 s, 1169 s, 1116 m, 1098 m, 1067 m, 1026 vs, 989 sh, 918 s, 840 s, 805 s, 732 s, 696 vs.

*2.2.3. Synthesis of $(VO(O_2PPh_2)_2)_\infty$ (**3**).* VO(acac)$_2$ (0.035 g, 0.133 mmol) and 0.058 g (0.266 mmol) of diphenylphosphinic acid were dissolved in 10 mL of methylene chloride and stirred overnight and resulted in 0.049 g of light blue **3**. Alternately, 0.0510 g (0.1923 mmol) of VO(acac)$_2$ and 0.0837 g (0.3846 mmol) of diphenylphosphinic acid were added to 5 mL of ethanol in a sealed tube and heated to 120 °C overnight. The light blue precipitate that had formed was filtered, rinsed with ethanol and then dried under vacuum to give 0.0580 g of light blue **3**. Both of these preparations resulted in species of identical IR spectra. Anal. Calc. for $C_{24}H_{20}O_5P_2V$: C, 57.50; H, 4.02. Found: C, 57.07; H, 3.94%. IR (Supporting Information Figure S5, neat, cm^{-1}): 3058 (vw), 1592 (vw), 1486 (vw), 1437 (m), 1124 (vs), 1057 (s), 1014 (s), 998 (m), 749 (m), 729 (s), 692 (s).

*2.2.4. Synthesis of $((H_2O)VO(O_2P(o\text{-}(CH_2)_2(C_6H_4))_\infty$ (**4**).* VO(acac)$_2$ (0.0402 g, 0.1516 mmol) and 0.0510 g (0.3033 mmol) of 2-hydroxyisophosphindoline-2-oxide were dissolved in 10 mL of methylene chloride and stirred overnight. The light blue precipitate that was produced was filtered off, rinsed with methylene chloride and then dried under vacuum to give 0.0330 g of compound **4**. Anal. Calc. for $C_{16}H_{18}O_6P_2V$: C, 45.84; H, 4.33. Found: C, 44.20; H, 3.87%. IR (Supporting Information Figure S6, neat, cm^{-1}): 3636 (vw), 3024 (vw), 2911 (vw), 1621 (vw), 1576 (vw), 1483 (w), 1458 (w), 1393 (w), 1267 (w), 1215 (s), 1197 (m), 1173 (s), 1153 (s), 1133 (w), 1094 (s), 1079 (s), 1062 (s), 1040 (vs), 1003 (s), 995 (vs), 950 (s), 854 (s), 818 (s), 796 (m), 760 (m), 735 (vs).

*2.2.5. Synthesis of $(VO(O_2P(o\text{-}(CH_2)_2(C_6H_4))_\infty$ (**5**).* VO(acac)$_2$ (0.0420 g, 0.1584 mmol) and 0.0533 g (0.3168 mmol) of 2-hydroxyisophosphin-doline-2-oxide acid were added to 5 mL of ethanol in a sealed tube and heated to 120 °C overnight. The light blue precipitate that had formed was filtered, rinsed with ethanol and then dried under vacuum to give 0.0460 g of compound **5**. Anal. Calcd for $C_{16}H_{16}O_5P_2V$: C, 47.90; H, 4.02. Found: C, 48.54; H, 4.36%. IR (Supporting Information Figure S7, neat, cm^{-}1): 3061 (vw), 2903 (vw), 1574 (vw), 1526 (vw), 1481 (w), 1455 (w), 1391 (w), 1295 (vw), 1221 (w), 1184 (s), 1178 (s), 1136 (vs), 1094 (vs), 1064 (vs), 1005 (vs), 881 (vw), 856 (s), 818 (m), 795 (m), 762 (m), 749 (s), 734 (s).

2.3. X-ray Crystallography. Suitable crystals were grown by a slow diffusion of hexanes into a saturated solution of either **1** or **2** in a 1:1 mixture of hexanes and methylene chloride in an H-tube. Diffraction data for all compounds were collected using a Bruker AXS SMART APEX CCD diffractometer using monochromatic Mo Kα radiation with the omega scan technique. Single crystals of compounds containing **1** and **2** were mounted on Mitegen micromesh supports using viscous oil flash-cooled to 100 K. Data were collected, unit cells

dx.doi.org/10.1021/ic201259u | Inorg. Chem. 2012, 51, 2766−2776

determined, and the data integrated and corrected for absorption and other systematic errors using the Apex2 suite of programs.[25] The structures were solved by direct methods and refined by full matrix least-squares against F^2 with all reflections using SHELXL.[26] Complex **1** cocrystallized with 3.5 dichloromethane molecules in the asymmetric unit with the entire contents of the crystal labeled as **A**. The dichloromethane molecules were not orderly arranged and the different disordered arrangements were adequately accounted for using standard models, see CIF file. Complex **1** within crystal **A** contained a 3-fold disorder consisting of the unique V-(OH_2) moiety occurring in three positions in unequal ratios as is illustrated in Figure 1. The disorder, readily apparent from the difference electron density maps during structure refinement, constitutes the only obvious way to rationalize the pattern obtained from the solution to the structure which looked like the combination figure of the three disordered patterns in Figure 1. Crystals for the study of complex **2**, where the entire contents of the crystal are labeled as **B**, were obtained via a different route to the one given above in the experimental details which affords analytically pure samples of **2**. This route, an exploratory reaction, consisted of reacting $VO(acac)_2(py)$ and dibenzylphosphinic acid (without any additional py) in a sealed tube with 5 mL of ethanol and heating at 120 °C for 16 h. In this case, the crystals **B** that were grown from this reaction (as described directly above) refined to represent a cocrystal of composition **2** and **1** in a 78.3(6):21.7(6) respective ratio. Evidence suggestive of the presence of **1** (smaller absorption at 3628 cm^{-1}, compared to the equivalent in Supporting Information Figure S3 of pure **1**) was observed in the FTIR spectrum of the crystals, Supporting Information Figure S8. One benzyl ligand also contained disorder. This was refined independently first to determine the occupancy ratio over the two sites and as this was similar to the composition of crystal **B**, it was then refined tied to the free variable that defined the occupancies of **2** and **1** in crystal **B**. The N atom (78.3(6)%) in the py ligand was refined with anisotropic thermal parameters and the O atom (21.7(6)%) in the ligated water molecule with isotropic parameters. The final Flack x parameter was −0.00(1) and for the inverted structure 0.96(2). We believe that the source of the water ligated in both crystal structures was the wet ethanol used in the synthesis. Pure crystals of **2** were grown by allowing slow diffusion of hexane into a dichloromethane solution of **2**. The final Flack *x* parameter was −0.02(1) and for the inverted structure 1.00(1). In all cases the final models consisted of non-H atoms represented by anisotropic displacement parameters and all H-atoms (including those on the aqua ligands in crystals **A** and **B**) were refined through constraints to the atoms they were bonded to. Details of the data collection and refinement of the compounds are given in Table 1.

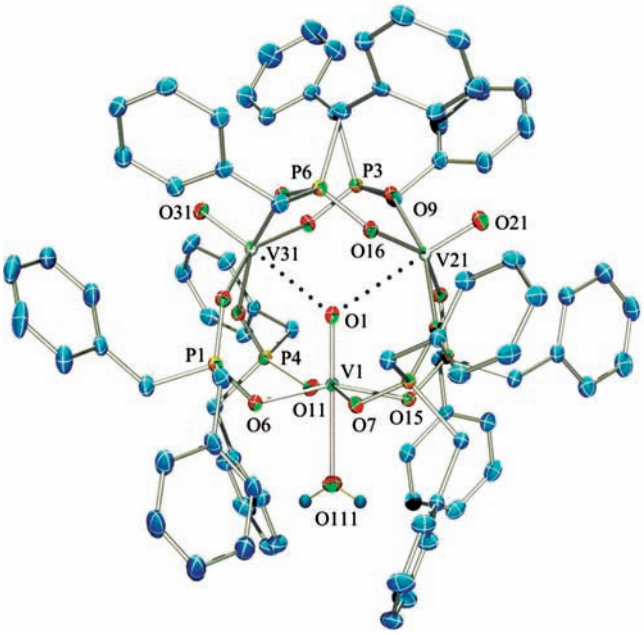

Figure 2. POV-Ray rendered drawing of an ORTEP-3[32] illustration of the major orientation of **1** within crystal **A**. Hydrogen atoms (except those on the aqua ligand, represented by spheres of arbitrary radii) have been omitted for clarity and the thermal ellipsoids are drawn at 30% probability. Dotted lines represent the long interactions between the central oxygen and the two vanadium atoms on the base.

3. RESULTS AND DISCUSSION

3.1. Synthesis. Compounds **1** and a mixture of **1** and **2** were prepared by heating two equivalents of dibenzylphosphinic acid with one equivalent of $VO(acac)_2$ or $VO(acac)_2(py)$ respectively in ethanol. The ligated water molecule in compound **1** is attributable to adventitious water in the ethanol which was not dried. The mixture of the pyridine and water adducts that was produced in the reaction employed to prepare compound **2**, as determined in crystal **B**, is also attributable to water being present in the ethanol. Here it is noteworthy that no peaks assignable to OH stretches were evident in the IR spectrum of the starting material $VO(acac)_2(py)$ and indeed $VO(acac)_2$ is known to contain a five coordinated vanadium atom.[24] Analytically pure **2** was made by mixing $VO(acac)_2$ with dibenzylphosphinic acid and adding a slight excess of pyridine in methylene chloride.

The IR spectra of compounds **1** and **2** (see Supporting Information Figures S3 and S4) contain peaks in the same regions with some notable differences. First complex **1** exhibits absorptions due to OH stretches at 3628 and 3537 cm^{-1} which are not evident in the spectrum for pure **2**. Second, there are subtle differences in the vanadium to oxygen atom stretching region where two bands at 1024 and 995 cm^{-1} for **1** and 1026 and 989 cm^{-1} for **2** are obtained. Perhaps facilitating assignment of these peaks is the fact that the VO stretch in $VO(acac)_2$ and $VO(acac)_2(py)$ comes at 993 and 964 cm^{-1} respectively, see Supporting Information Figures S1 and S2. Therefore the absorptions at 1024 and 1027 cm^{-1} can be assigned to the two "base" vanadium atoms containing terminal oxo ligands and the absorptions at 995 and 989 cm^{-1} in **1** and **2** respectively to the "vertex" VO bond located trans to the aqua and pyridine ligands.

The reactions with diphenylphosphinic acid or 2-hydroxyisophosphindoline-2-oxide used in place of dibenzylphosphinic acid using the same procedure conducted to produce **1**, resulted in blue intractable precipitates that proved to be insoluble in most common organic solvents as was detailed previously for diphenylphosphinate complexes with zirconium, vanadium and molybdenum.[28] Reactions consisted either of stirring at room temperature in CH_2Cl_2 or heating the reactants in EtOH at 120 °C. In the case of diphenylphosphinic acid, seemingly identical products assigned on the basis of elemental analysis as $(VO(O_2PPh_2)_2)_\infty$, **3**, were obtained based on a comparison of the IR spectra, Supporting Information Figure S5. It should be noted that this IR spectrum for **3** differs substantially from that reported previously[28] but similar thermal stabilities were found with an 8% weight lost (Supporting Information Figure S10) over the temperature range of 300−400 °C compared to the reported loss of 10.3%.[28]

In the case of 2-hydroxyisophosphindoline-2-oxide, the complex $((H_2O)VO(O_2P\text{-}o\text{-}(CH_2)_2C_6H_4)_2)_\infty$, **4**, was produced when the reactants were stirred at room temperature in CH_2Cl_2 (which was not dried), and, $(VO(O_2P(o\text{-}(CH_2)_2(C_6H_4))_\infty$, **5** was obtained when the reaction was conducted at 120 °C in EtOH. These assignments are based on elemental analyses. The IR spectra for **4** (Supporting Information Figure S6) contained

dx.doi.org/10.1021/ic201259u | Inorg. Chem. 2012, 51, 2766−2776

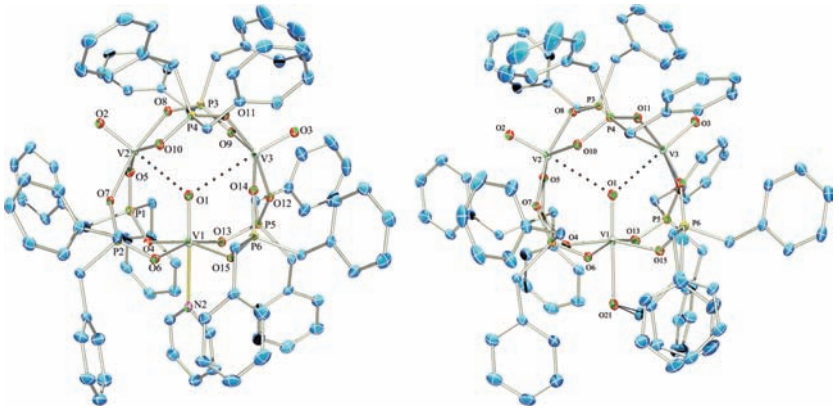

Figure 3. POV-Ray rendered drawings of ORTEP-3[32] representations of complex **2** (left, 78.3(6)%) and **1** (right, 21.7(6)%) which cocrystallized in the form of crystal **B**. Hydrogen atoms (except those on the aqua ligand, represented by spheres of arbitrary radii) have been omitted for clarity and the thermal ellipsoids are drawn at 30% probability. Dotted lines represent the long interactions between the central oxygen and the two vanadium atoms on the base.

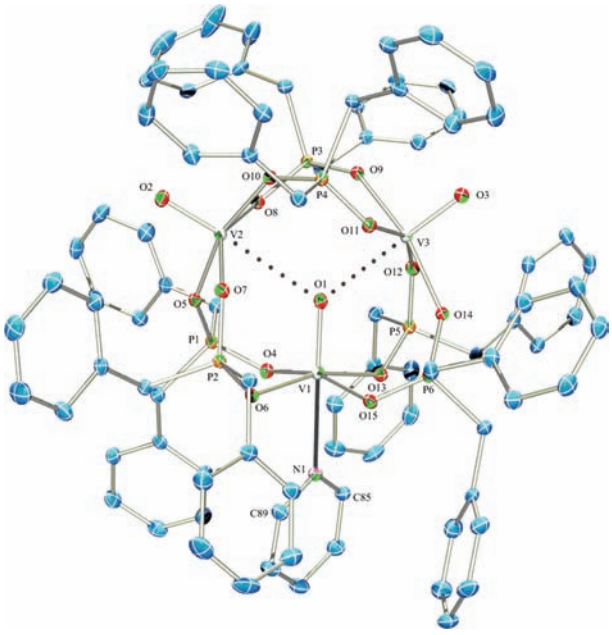

Figure 4. POV-Ray rendered drawings of ORTEP-3[32] representations of pure complex **2**. Hydrogen atoms have been omitted for clarity and the thermal ellipsoids are drawn at 30% probability. Dotted lines represent the long interactions between the central O and the two vanadium atoms on the base.

a stretch at 3636 $cm^{-1,}$ which is indicative of a ligated water molecule whereas that for **5** (Supporting Information Figure S7) did not contain absorptions in the 3600 cm^{-1} region. Also noteworthy was the fact that the fingerprint regions of these FTIR spectra for complexes **3**-**5** were considerable different than those obtained for **1** and **2** in that strong absorptions around the 995 and 1025 cm^{-1} region were not present. These would be indicative of a nonclassical $[(V_3(\mu_3\text{-}O)O_2)]^{6+}$ moiety as described above. These insoluble products may be in the form of large clusters and/or polymers[29−31] but this is somewhat speculative.[19] For additional identification purposes the X-ray powder diffraction pattern for these compounds is presented as Supporting Information Figure S9, and these revealed dramatically different patterns between compounds $((H_2O)VO(O_2Po\text{-}(CH_2)_2C_6H_4)_2)_\infty$, **4** and $(VO(O_2P(o\text{-}(CH_2)_2\text{-}(C_6H_4))_\infty$, **5**. It is somewhat difficult to account for this difference in the reaction products for the different phosphinic acids, though the lower solubility and the larger steric effects of the dibenzylphosphinate ligand may be contributing factors leading to the trimers.

3.2. Crystallography. Crystals studied were obtained from saturated 1:1 solutions of hexanes and methylene chloride layered with more hexanes. Crystals were shaped as flat plates and colored light blue. Compound **1** crystallized as a solvate with four molecules of **1** and fourteen molecules of CH_2Cl_2 in the unit cell of crystal **A**. Complex **1** of formulation $(V_3(\mu_3\text{-}O)O_2)(\mu_2\text{-}O_2P(CH_2C_6H_5)_2)_6(H_2O)$, has the three vanadium atoms in the "$(VO)_3$" moiety forming a triangle with one oxo bond roughly in the center of the quasi-isosceles triangle (C_{2v} symmetry) and the other two oxo ligands outside with one on each vanadium atom. The outer periphery of complex **1**, namely the six bridging benzyl phosphinate ligands did not contain disorder, but the inner "$V_3(\mu_3\text{-}O)O_2)(H_2O)$" unit was refined to occupy three non equal sites with 60.6(6):31.3(5):7.7(2) occupancies as illustrated in Figure 1. In this formation, each vanadium atom is six coordinated (distorted octahedral). Two of the three vanadium atoms are coordinated in a pseudo-octahedral fashion to an outward pointing oxo ligand, four O atoms from the four bridging phosphinate ligands and at long distances of 2.74(20 and 2.57(2) Å to the central oxygen atom; the third vanadium atom is coordinated to one outward pointing aqua ligand and double bonded to the central O atom (1.60(2) Å) completing the octahedral coordination spheres as illustrated in Figure 2, which shows the major orientation. Our first attempt at obtaining the crystal structure of complex **2** revealed a cocrystal consisting of **2** and **1** in a 78.3(6):21.7(6) respective ratio described here as crystal **B** and **2** was then more deliberately crystallized in pure form. Drawings of the two complexes in crystal **B** are depicted in Figure 3 and that for pure **2** is given in Figure 4. Tables 2 and 3 list selected bond distances and angles for **1** and **2** as defined in crystal **B** and pure **2**. Table 4 contains a comparison of the three different refined triangular arrangements in complexes **1**, pure **2**, and that for the previously reported $(V_3(\mu_3\text{-}O)O_2)(C_6H_5CO_2)_6(THF)$, **6**,[19] and related $[(V_3(\mu_3\text{-}O)O_2)((C_2H_5O)_2PO_2)_6\cdot CH_3CN]$, **7**.[5] In all cases, significantly different distances for the two long interactions between the interstitial oxygen atom to two vanadium atoms on the base were present, see rows 3 and 4 in Table 2. This asymmetry was utilized in producing the overlay diagrams since this allowed for the alignment of the "V_3" triangles and all the

dx.doi.org/10.1021/ic201259u | *Inorg. Chem.* 2012, 51, 2766−2776

Table 2. Selected Bond Distances for Major Components, That Is, Major Orientation for 1 and 2 from Crystal B and Pure 2[a]

bond distances (Å)					
compound **1**		**2** from crystal **B**		pure **2**	
V(1)−O(1)	1.600(17)	V(1)−O(1)	1.619(3)	V(1)−O(1)	1.625(2)
V(31)−O(1)	2.57(2)	V(2)−O(1)	2.487(3)	V(2)−O(1)	2.510(2)
V(21)−O(1)	2.74(2)	V(3)−O(1)	2.837(2)	V(3)−O(1)	2.830(3)
V(2)−O(2)	1.63(2)	V(2)−O(2)	1.581(2)	V(2)−O(2)	1.588(2)
V(3)−O(3)	1.58(9)	V(3)−O(3)	1.587(2)	V(3)−O(3)	1.584(2)
V(1)−O(7)	1.942(3)	V(1)−O(15)	2.010(2)	V(1)−O(13)	2.019(2)
V(1)−O(11)	1.962(3)	V(1)−O(4)	1.997(3)	V(1)−O(4)	1.988(2)
V(1)−O(6)	1.985(3)	V(1)−O(6)	1.981(2)	V(1)−O(6)	2.010(2)
V(1)−O(15)	2.024(3)	V(1)−O(13)	1.974(2)	V(1)−O(15)	1.984(2)
V(21)−O(21)	1.562(4)	V(3)−O(3)	1.587(2)	V(3)−O(3)	1.584(2)
V(21)−O(14)	1.979(3)	V(3)−O(14)	1.981(2)	V(3)−O(14)	1.999(2)
V(21)−O(8)	1.979(3)	V(3)−O(12)	1.986(2)	V(3)−O(12)	1.984(2)
V(21)−O(9)	1.997(3)	V(3)−O(9)	1.967(2)	V(3)−O(9)	2.003(2)
V(21)−O(16)	1.999(3)	V(3)−O(11)	1.988(2)	V(3)−O(11)	1.971(2)
V(31)−O(31)	1.572(3)	V(2)−O(2)	1.581(3)	V(2)−O(2)	1.588(2)
V(31)−O(10)	1.986(3)	V(2)−O(8)	2.010(2)	V(2)−O(8)	1.989(2)
V(31)−O(13)	1.992(3)	V(2)−O(5)	1.986(3)	V(2)−O(5)	2.024(2)
V(31)−O(5)	1.999(3)	V(2)−O(7)	2.024(2)	V(2)−O(7)	1.993(2)
V(31)−O(12)	2.003(3)	V(2)−O(10)	1.984(2)	V(2)−O(10)	2.019(2)
O(5)−P(1)	1.511(3)	P(1)−O(5)	1.505(3)	P(1)−O(5)	1.513(2)
O(6)−P(1)	1.501(3)	P(1)−O(4)	1.513(3)	P(1)−O(4)	1.518(2)
O(7)−P(2)	1.517(3)	P(2)−O(7)	1.495(3)	P(2)−O(7)	1.516(2)
O(8)−P(2)	1.511(3)	P(2)−O(6)	1.507(3)	P(2)−O(6)	1.516(2)
O(9)−P(3)	1.508(3)	P(3)−O(8)	1.502(2)	P(3)−O(8)	1.523(2)
O(10)−P(3)	1.522(3)	P(3)−O(9)	1.514(2)	P(3)−O(9)	1.516(2)
O(11)−P(4)	1.513(3)	P(4)−O(11)	1.514(2)	P(4)−O(11)	1.524(2)
O(12)−P(6)	1.507(3)	P(4)−O(10)	1.517(3)	P(4)−O(10)	1.506(2)
O(13)−P(4)	1.500(3)	P(5)−O(12)	1.510(2)	P(5)−O(12)	1.522(2)
O(14)−P(5)	1.503(3)	P(5)−O(13)	1.518(2)	P(5)−O(13)	1.515(2)
O(15)−P(5)	1.518(3)	P(6)−O(15)	1.509(3)	P(6)−O(15)	1.521(2)
O(16)−P(6)	1.516(3)	P(6)−O(14)	1.512(3)	P(6)−O(14)	1.514(2)
		V(1)−N(2)	2.331(11)	V(1)−N(1)	2.350(3)
		N(2)−C(13)	1.232(10)	N(1)−C(85)	1.339(4)
		N(2)−C(17)	1.434(12)	N(1)−C(89)	1.353(4)
V(1)−O(111)	2.307(4)	V(1)−O(21)	2.24(3)		

[a]Equivalent distances are on the same horizontal line.

equivalent distances noted in Tables 2 and 3 were based on this alignment. The fact that an examination of the equivalent bond distances and angles for the three arrangements of the inner core of complex **1** are not that significantly different suggests that the model is accurate and that benzylphosphinate ligands have great flexibility in stabilizing the inner core geometries. The flexibility is demonstrated in the fact that an overlay of the two V_3 triangular cores in **1** from crystal **A** and **2** from crystal **B** reveals different arrangements of the benzyl groups as illustrated in Figure 5. Interestingly these differences in benzyl group arrangements are more pronounced in an overlay between complex **2** from crystal **B** and pure **2** as illustrated in Figure 5. This suggests that the cocrystallization of 78.3(6)% of **2**:21.7(6)% of **1** resulted in a packing arrangement which differs substantially from that occurring in pure **2** which would imply that any differences in bond lengths and angles noted in Tables 2 and 3 may partly be as a result of the cocrystallization in crystal **B** but more likely the different internal ligand arrangements. As can be seen in Figure 6, the py ligand plane in crystal **B** in these two structures is oriented almost parallel to the O4−V1−O15 plane in **2** from crystal **B** whereas the py plane is rotated 90° and is almost parallel to the O6−V1−O13 plane in pure **2**. While these different orientations of the py ligand in these two molecules result in the interesting fact that the overall geometries depicted in Figure 6 appear as mirror images, it is the main reason why some of the equivalent bond angles listed in Table 6 are significantly different.

The nature of the disorder in crystal **A** reduced the accuracy with which some of the distances in the different orientations of **1** could be refined and, in particular, the nature of the interstitial oxygen atom was not determined accurately as reflected in the number of decimal places (i.e., 2 and not 3) for data associated with the atoms labeled as O(1), O(2), and O(3) and only a listing of the two major orientations for **1** is given in Table 4. This suffices to demonstrate equivalency and merit in the refinement and we restrict a comparison in distances to 60.6% **1** and **2** as detailed in Table 4 and some conclusions can be drawn as follows:

1. There are no discernible significant differences in the vanadium to interstitial oxygen atom and the other two vanadium to O_{oxo} atom distances in **1**, namely V(1)−O(1) = 1.60(2) Å, V(21)−O(21) = 1.562(3) Å and V(31)−O(31) = 1.572(3) Å for **1**. The equivalent distances, that is, V to $O_{central}$ compared to V to $O_{terminal}$ in **2**, **6** and **7** (situated on a crystallographic 2-fold axis) are significantly different presumably as a result of the ligand trans to the central O atom. It is likely that the disorder in **1**, that is, this one oxygen atom (O(1) + O(2) + O(3) = 100% O in **1**) was refined over three different positions, prevented accurate resolution.
2. The vanadium to oxygen atom distance in the aqua ligand in **1** (2.307(4) Å) is comparable with the equivalent distance for **1** in crystal **B** at 2.24(3) Å and the vanadium to nitrogen atom in pyridine in **2** from crystal **B** (2.331(11) Å) is equivalent to that in pure **2** at 2.350(2) Å. However, the vanadium to oxygen atom

dx.doi.org/10.1021/ic201259u | Inorg. Chem. 2012, 51, 2766−2776

Table 3. Selected Bond Angles for 1 (Major Orientation), 2 from Crystal B, and Pure 2[a]

bond angles (deg)					
compound 1		2 from crystal B		pure 2	
O(1)–V(1)–O(7)	98.8(7)	O(1)–V(1)–O(15)	99.39(11)	O(1)–V(1)–O(15)	98.40(10)
O(1)–V(1)–O(11)	97.1(7)	O(1)–V(1)–O(4)	96.39(11)	O(1)–V(1)–O(4)	98.79(10)
O(7)–V(1)–O(11)	164.05(19)	O(4)–V(1)–O(15)	164.21(10)	O(4)–V(1)–O(15)	162.81(9)
O(1)–V(1)–O(6)	101.0(6)	O(1)–V(1)–O(6)	98.72(11)	O(1)–V(1)–O(6)	96.14(10)
O(7)–V(1)–O(6)	89.10(12)	O(6)–V(1)–O(15)	87.94(10)	O(6)–V(1)–O(15)	89.05(9)
O(11)–V(1)–O(6)	89.30(12)	O(6)–V(1)–O(4)	89.22(10)	O(6)–V(1)–O(4)	89.39(9)
O(1)–V(1)–O(15)	101.4(6)	O(1)–V(1)–O(13)	98.47(11)	O(1)–V(1)–O(13)	99.39(10)
O(7)–V(1)–O(15)	88.27(11)	O(13)–V(1)–O(15)	88.95(10)	O(13)–V(1)–O(15)	89.02(9)
O(11)–V(1)–O(15)	87.19(12)	O(13)–V(1)–O(4)	89.19(10)	O(13)–V(1)–O(4)	87.92(9)
O(6)–V(1)–O(15)	157.65(18)	O(13)–V(1)–O(6)	162.81(11)	O(13)–V(1)–O(6)	164.46(9)
O(1)–V(1)–O(111)	179.8(9)	O(1)–V(1)–N(2)	179.4(3)	O(1)–V(1)–N(1)	176.95(10)
O(7)–V(1)–O(111)	81.33(13)	O(15)–V(1)–N(2)	81.2(3)	O(15)–V(1)–N(1)	79.94(9)
O(11)–V(1)–O(111)	82.79(14)	O(6)–V(1)–N(2)	81.1(3)	O(6)–V(1)–N(1)	81.30(9)
O(6)–V(1)–O(111)	79.14(13)	O(4)–V(1)–N(2)	83.0(3)	O(4)–V(1)–N(1)	82.89(9)
O(15)–V(1)–O(111)	78.52(13)	O(13)–V(1)–N(2)	81.7(3)	O(13)–V(1)–N(1)	83.18(9)
O(21)–V(21)–O(14)	104.77(15)	O(3)–V(3)–O(12)	98.58(11)	O(3)–V(3)–O(12)	105.16(11)
O(21)–V(21)–O(8)	100.53(15)	O(3)–V(3)–O(14)	105.25(12)	O(3)–V(3)–O(14)	98.26(11)
O(14)–V(21)–O(8)	89.59(11)	O(14)–V(3)–O(12)	89.59(10)	O(14)–V(3)–O(12)	89.55(9)
O(21)–V(21)–O(9)	98.29(15)	O(3)–V(3)–O(9)	106.30(12)	O(3)–V(3)–O(9)	99.03(11)
O(14)–V(21)–O(9)	85.72(11)	O(9)–V(3)–O(12)	86.69(10)	O(9)–V(3)–O(12)	86.66(9)
O(8)–V(21)–O(9)	161.17(15)	O(9)–V(3)–O(14)	148.44(10)	O(9)–V(3)–O(14)	162.69(9)
O(21)–V(21)–O(16)	105.54(15)	O(3)–V(3)–O(11)	98.98(11)	O(3)–V(3)–O(11)	106.26(11)
O(14)–V(21)–O(16)	149.55(15)	O(12)–V(3)–O(11)	162.43(9)	O(12)–V(3)–O(11)	148.57(9)
O(8)–V(21)–O(16)	87.73(11)	O(14)–V(3)–O(11)	86.50(10)	O(14)–V(3)–O(11)	86.87(9)
O(9)–V(21)–O(16)	87.14(11)	O(9)–V(3)–O(11)	87.71(10)	O(9)–V(3)–O(11)	87.58(9)
O(31)–V(31)–O(10)	104.09(14)	O(2)–V(2)–O(8)	95.89(11)	O(2)–V(2)–O(8)	103.11(11)
O(31)–V(31)–O(13)	98.07(13)	O(2)–V(2)–O(5)	102.06(12)	O(2)–V(2)–O(5)	97.10(10)
O(10)–V(31)–O(13)	86.98(11)	O(5)–V(2)–O(8)	86.82(10)	O(5)–V(2)–O(8)	88.87(9)
O(31)–V(31)–O(5)	103.55(13)	O(2)–V(2)–O(7)	97.03(11)	O(2)–V(2)–O(7)	102.12(11)
O(10)–V(31)–O(5)	152.36(12)	O(8)–V(2)–O(7)	166.93(10)	O(8)–V(2)–O(7)	154.77(9)
O(13)–V(31)–O(5)	88.63(11)	O(5)–V(2)–O(7)	88.60(10)	O(5)–V(2)–O(7)	88.45(9)
O(31)–V(31)–O(12)	97.73(13)	O(2)–V(2)–O(10)	103.42(12)	O(2)–V(2)–O(10)	95.83(10)
O(10)–V(31)–O(12)	89.86(11)	O(10)–V(2)–O(8)	90.13(10)	O(10)–V(2)–O(8)	90.47(9)
O(13)–V(31)–O(12)	164.19(11)	O(10)–V(2)–O(5)	154.52(10)	O(10)–V(2)–O(5)	166.86(9)
O(5)–V(31)–O(12)	87.00(11)	O(10)–V(2)–O(7)	88.75(10)	O(10)–V(2)–O(7)	86.56(9)

[a]Equivalent angles are on the same horizontal line.

distances in **1** are significantly longer than the vanadium to O_{THF} atom distance in **6** at 2.186(6) Å whereas the vanadium to N(py) distances in **2** are equivalent to the vanadium to N atom in acetonitrile in **7** at 2.352(6) Å.

3. The lengths of the sides of the "V_3" quasi-isosceles triangle in **1** (3.830(3), 3.742(2), 4.422(2) Å) and pure **2** (3.917(1), 3.738(1), 4.409(1) Å) are significantly larger than those in **6** (3.520(2), 3.572(2), 4.050(2) Å), and shorter than those in **7** (3.926(2) and 4.540(2) Å), see Table 4. This can be attributed to the larger chelating capabilities of the phosphinate ligand as compared with that of the carboxylate moieties in **6** as noted previously.[2]
4. The interstitial O atom, O(1), is displaced more from the center of the quasi-isosceles triangle formed by the three vanadium atoms in **2** compared to **1** judging by the V(2)–O(1) and V(3)–O(1) labeled distances in **2**. The fact that the equivalent distances are shorter in **6** may be attributed to the shorter triangle. The three interstitial angles add up to exactly 360° for **1** and **2** thus proving the planarity of the core.
5 The bond distances between the vanadium and the O atom on the aqua ligand in both **1** from crystals **A** and **B** at 2.307(4) and 2.24(3) Å are suggestive of a long single bond and it is noteworthy that there are no hydrogen bonds associated with this coordinated water molecule, presumably due to steric shielding by the bulky benzyl groups. Apart from the coordination by the O atom, the environment of the two H atoms being surrounded by phenyl groups is similar to that in the recently reported $H_2O@C_{60}$ where a single water molecule was encapsulated by C_{60}.[35]

In light of this analysis and that previously reported for **6**,[19] the structures of related trinuclear vanadium complexes both which contained disorder and were assigned by crystallography as cocrystals consisting of $[(C_2H_5)_2NH_2]_2[\{V^{4+}O(\mu_2\text{-}H_2L)\}_3(\mu_3\text{-}O)]_{0.67}[\{V^{4+}(OH)(\mu_2\text{-}HL)\}_3(\mu_3\text{-}O)]_{0.33}\cdot 2H_2O$, where H_4L = $CH_3C(OH)PO_3H_2)_2$,[36] and, $\{[V_3O_3(OH)(H_2hedp)(Hhedp)_2]^{6-}\}$[37] where H_5hedp = etidronic acid, may be in need of reassignment.

3.3. Magnetic Susceptibility Measurements. The magnetic moments of compounds **1**–**5** were measured at 296K in triplicate and are listed in Table 5 with raw data as Supporting Information Table S1. Compounds **1** and **2** display magnetic moments for three oxovanadium d^1 centers contained

dx.doi.org/10.1021/ic201259u | Inorg. Chem. 2012, 51, 2766–2776

Table 4. Comparison of Core Geometric Parameters in $(V_3(\mu_3\text{-}O)O_2)(\mu_2\text{-}O_2P(CH_2C_6H_5)_2)_6H_2O$, 1, $(V_3(\mu_3\text{-}O)O_2)(\mu_2\text{-}O_2P(CH_2C_6H_5)_2)_6py$, pure 2, $(V_3(\mu_3\text{-}O)O_2)(C_6H_5CO_2)_6(THF)$, 6[19], and $[(V_3(\mu_3\text{-}O)O_2)((C_2H_5O)_2PO_2)_6{\cdot}CH_3CN]$, 7[5]

60.6% **1**, Figure 1		31.3% **1**, Figure 1		Pure **2**, Figure 4		**6**		**7**	
				distances (Å)					
V(1)−O(1)	1.60(2)	V(2)−O(2)	1.63(3)	V(1)−O(1)	1.625(2)	V(1)−O(10)	1.626(6)	V(1)−O(1)	1.623(4)
V(21)−O(21)	1.562(3)	V(11)−O(111)	1.576(4)	V(2)−O(2)	1.588(2)	V(2)−O(8)	1.582(5)	V(2)−O(2)	1.584(3)
V(31)−O(31)	1.572(3)	V(31)−O(31)	1.572(3)	V(3)−O(3)	1.584(2)	V(3)−O(9)	1.568(6)		
V(1)−O(111)	2.307(4)	V(2)−O(21)	2.324(5)	V(1)−N(1)	2.350(2)	V(1)−O(7)	2.186(6)	V(1)−N(1)	2.352(6)
V(21)−O(1)	2.74(2)	V(11)−O(2)	2.65(3)	V(2)−O(1)	2.510(2)	V(2)−O(10)	2.344(7)	V(2)−O(1)	2.765(3)
V(31)−O(1)	2.57(2)	V(31)−O(2)	2.60(3)	V(3)−O(1)	2.830(3)	V(3)−O(10)	2.452(6)		
V(1)···V(21)	3.830(3)	V(2)···V(11)	3.825(5)	V(1)···V(3)	3.917(1)	V(1)···V(2)	3.520(2)		
V(1)···V(2)		3.926(2)[a]							
V(1)···V(31)	3.742(2)	V(2)···V(31)	3.738(4)	V(1)···V(2)	3.738(1)	V(1)···V(3)	3.572(2)		
V(21)···V(31)	4.422(2)	V(11)···V(31)	4.374(3)	V(2)···V(3)	4.409(1)	V(2)···V(3)	4.050(2)	V(2)···V(2′)	4.540(2)[a]
				bond angles (deg)					
O(1)−V(1)−O(111)	179.8(6)	O(2)−V(2)−O(21)	177(1)	O(1)−V(1)−N(1)	176.95(10)	O(10)−V(1)−O(7)	179.2(3)	O(1)−V(1)−N(1)	180(2)
V(1)−O(1)−V(21)	121.6(8)	V(2)−O(2)−V(31)	122(1)	V(1)−O(1)−V(3)	120.7(1)	V(1)−O(10)−V(2)	123.9(3)		
V(1)−O(1)−V(31)	125.8(9)	V(2)−O(2)−V(11)	125(1)	V(1)−O(1)−V(2)	128.1(1)	V(1)−O(10)−V(3)	120.9(3)	V(1)−O(1)−V(2)	125(2)
V(21)−O(1)−V(31)	112.6(6)	V(11)−O(2)−V(31)	113(1)	V(2)−O(1)−V(3)	111.15(9)	V(2)−O(10)−V(3)	115.2(2)	V(2)−O(1)−V(2′)	110.3(1)[a]
V(21)−V(1)−V(31)	71.45(4)	V(11)−V(2)−V(31)	70.66(7)	V(2)−V(1)−V(3)	70.28(2)	V(2)−V(1)−V(3)	69.65(4)	V(2)−V(1)−V(3)	70.66(3)[a]
V(1)−V(31)−V(21)	55.20(3)	V(2)−V(31)−V(11)	55.61(6)	V(1)−V(3)−V(2)	52.95(1)	V(1)−V(3)−V(2)	54.57(4)	V(1)−V(2)−V(2′)	54.67(3)[a]
V(1)−V(21)−V(31)	53.35(3)	V(2)−V(11)−V(31)	53.73(6)	V(1)−V(2)−V(3)	56.7(1)	V(1)−V(2)−V(3)	55.78(4)	V(1)−V(2)−V(3)	

[a]As indicated, some distances for 7 were obtained using Mercury[33] and the data code named NEJCUA available on the CCDC.[34]

dx.doi.org/10.1021/ic201259u | Inorg. Chem. 2012, 51, 2766−2776

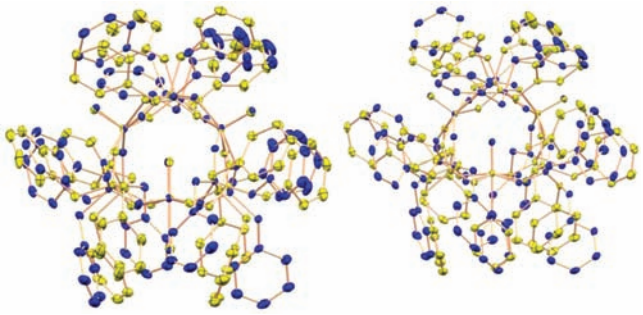

Figure 5. POV-Ray rendered Mercury[33] produced overlay of the "(V_3)" cores of the major orientation of **1** (light or yellow) in crystal **A** and the H_2O adduct (dark or blue) in crystal **B** on the left and an overlay of **2** from crystal **B** (light or yellow) and that of pure **2** (dark or blue).

in one molecule and the variable temperature measurement on complex **2**, Figure 7, suggests that there is a very weak interaction between the vanadyl centers in this molecule.

The data (susceptibility versus temperature and magnetization versus field) were simultaneously simulated with MAGPACK,[38] using the same set of parameters: g = 1.98, J = +0.64 cm^{-1}, and J' = −0.61 cm^{-1} for the Hamiltonian: $H = -2J(S_1S_2 + S_2S_3) - 2J'S_1S_3$. The very weak exchange interactions are consistent with the crystal structure and the long V···V distances.

This is in contrast to the data reported for the antiferromagnetically coupled vanadium(IV) dimer $[V_2O_2(\mu\text{-OH})(\mu\text{-SO}_4)([9]aneN_3)_2]Br_2$ of 1.2 μ_B[39] at 293 K and for the anionic cluster $[(VO)_2BP_2O_{10}]_6^{18-}$ of 1.59 μ_B[40] at 298 K, which both contain shorter V···V distances. The magnetic moments for polymeric species **3**−**5** were similar to the spin-only moment for an unpaired d^1 electron as was noted for molecular vanadium(IV) species.[41,42] Previous measurements with oxovanadium dimers in which two or three diphenylphosphinate ligands bridged two vanadium centers resulted in magnetic moments at room temperature close to the spin-only moment for one unpaired electron.[9,11,43] Additionally, a 2-dimensional oxovanadium phosphinate polymer was also reported to have a magnetic moment near the spin-only moment for one unpaired electron.[12] In each case, the vanadium centers are connected to each other by bridging phosphinate ligands but show no substantial magnetic interaction.

3.4. Thermal Analysis. The TGA for $VO(acac)_2$, Supporting Information Figure S11, and TGA and DSC for $VO(acac)_2(py)$,

Table 5. Magnetic Moments of Oxovanadium Phosphinate Compounds

compound	$\mu_{eff}{}^a/\mu_B$
1	3.02(1)
2	3.045(6)
3	1.76(2)
4	1.758(7)
5	1.77(3)

[a]All measurements conducted in triplicate at 296K.

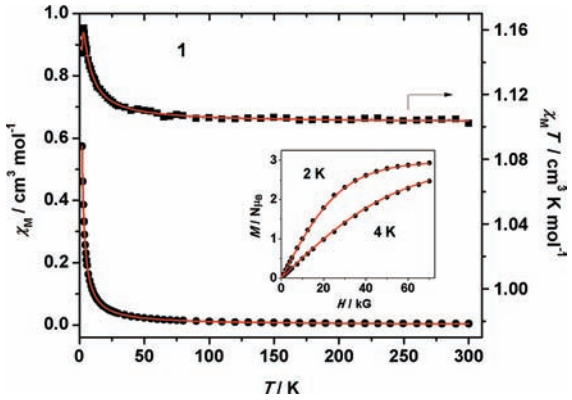

Figure 7. Measured and calculated χ_M and $\chi_M T$ against T for compound X. Inset: M vs H for compound X at 2 and 4 K. The lines are the best fit of the data using the parameters described in the text.

Supporting Information Figures S12 and S13, have been previously reported,[41,44] and we remeasured these as a check of instrumental accuracy. The results suggest (based solely upon color and weight loss) that both $VO(acac)_2$ and $VO(acac)_2(py)$ decompose to V_2O_3 by 270 °C and the pathway with $VO(acac)_2(py)$ includes the loss of pyridine (calc. 23.0%; obs. 21.6%), Supporting Information Figure S12. DSC suggests that the absorption of 58.0 kJ/mol is required to break the vanadium to N_{py} bond in $VO(acac)_2(py)$, Supporting Information Figure S13, which is comparable to the 69.4 kJ/mol previously reported.[44] $VO(acac)_2$ and $VO(acac)_2(py)$ presented 74.1% and 80.2% weight losses, which are higher than the expected values of 71.7% and 78.1% for a V_2O_3 residue possibly because of sublimation of $VO(acac)_2$, Supporting Information Figures S11−S12.

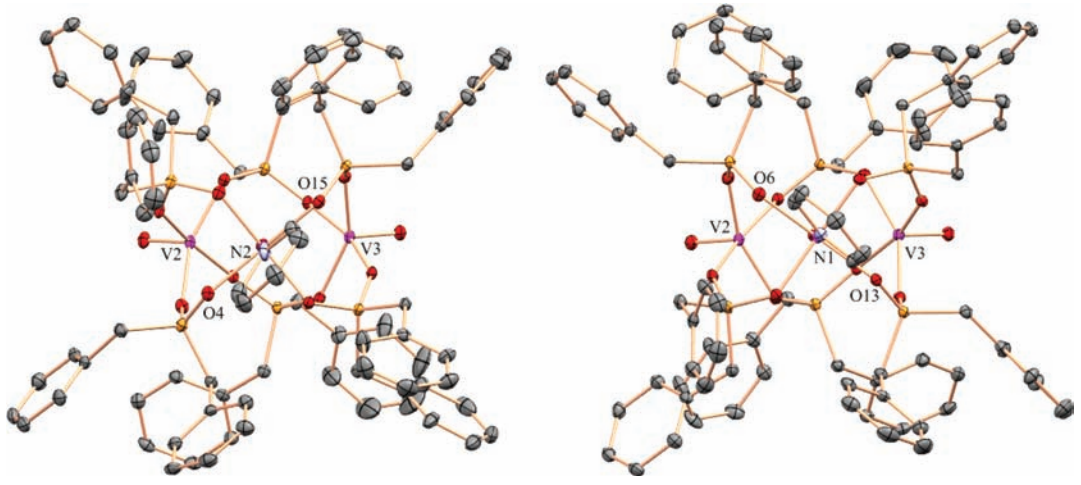

Figure 6. POV-Ray rendered Mercury[33] produced illustration of **2** from crystal **B** (left) and pure **2** (right) with the V2 and V3 atoms located in similar positions depicting the different orientation of the py ligands.

dx.doi.org/10.1021/ic201259u | Inorg. Chem. 2012, 51, 2766−2776

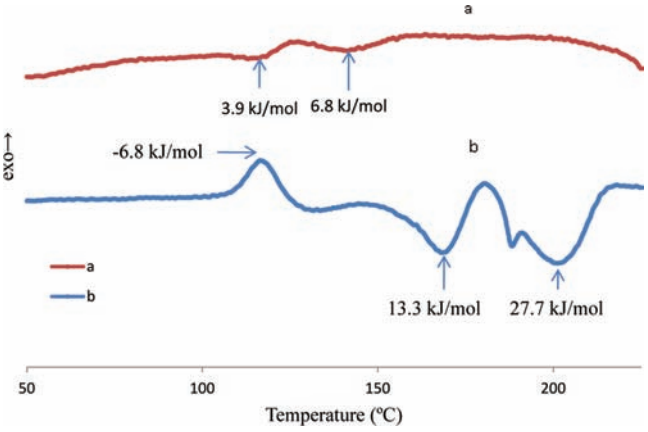

Figure 8. DSC thermograms (5 °C min^{-1}, N_2 atmosphere) for **1** (a, top curve) and **2** (b, bottom curve).

Sublimation of $VO(acac)_2$ was thought not to occur under these conditions[45] but more recent work suggests otherwise.[46]

In order to understand the TGA data of the complexes produced we measured that for the ligand dibenzylphosphinic acid which is reproduced as Supporting Information Figure S14. This revealed a loss in weight of 82.0% from 250 to 400 °C corresponding to the decomposition of the ligand and possibly the production of P_2O_3. The TGA of **1**, Supporting Information Figure S15, indicated a loss of ligated water starting at 100 °C (calc. 1.1%; obs. 1.7%), followed by a weight loss over the 300−400 °C range (obs. 12.1%). A bulk study where we obtained an IR spectrum of the dissociated material revealed that this was dissociated ligand. At 500 °C the complex decomposed further and, in this run, the sample was heated to 600 °C and kept at this temperature for 30 min, Supporting Information Figure S15a. The TGA of **2**, Supporting Information Figure S16, conducted in a similar manner to that for **1**, revealed a weight loss corresponding to pyridine (calcd 5.2%; obsd 4.5%) and then presumably some ligand dissociation (obs. 11.7%) followed by decomposition with heating up to 600 °C for 30 min, Supporting Information Figure S16a. The FTIR spectra of the final products obtained after heating **1** and **2** up to 600 °C were identical and similar to that for complex **1**, Supporting Information Figure S17, and are comparable to that reported after heating V_2O_5−P_2O_5 (in the P/V ratio = 2) which was mostly $VO(PO_3)_2$.[47] While the thermolysis of $(VO)_3((C_2H_5O)_2PO_2)_6{\cdot}CH_3CN$ was reported to produce $VO(PO_3)_2$,[5] in our studies on **1** and **2** loss of dissociated ligand would prevent this compound from being produced in a pure state. An X-ray powder diffraction measurement on this residue product was not conclusive as the compound was amorphous.

The DSC of **1** contained two small absorptions at 120 and 140 °C corresponding to 3.9 and 6.8 kJ/mol and a melting transition at 240 °C of 60.7 kJ/mol, Supporting Information Figure S1. The DSC of **2** revealed a crystallization process at 120 °C corresponding to the release of 6.8 kJ/mol and two absorptions at 170 and 200 °C (also contains a shoulder blip) of 13.3 and 28.7 kJ/mol, respectively, followed by a melting transition at 240 °C of 65.2 kJ/mol, Supporting Information Figure S19. These two plots (without the melting transitions) are illustrated in Figure 8. We believe that some sort of reorganization is taking place in these complexes that prevents the sharp rupture and dissociation of the H_2O and pyridine ligands in **1** and **2** respectively. Evidence for this is present in the crystallization of **2** in the DSC plot and the fact that the TGA only indicated weight loss for the H_2O and pyridine ligands in **1** and **2** up to 280 °C. Therefore it is reasonable to consider the absorptions of the sum of the two peaks for **1** at 120 and 140 °C of 10.7 kJ/mol and that for **2** at 170 and 200 °C equal to 42.0 kJ/mol as corresponding to the energies required to liberate the vanadium to O_{water} bond in **1** and the vanadium to N_{py} bond in **2**. It did require 58.0 kJ/mol for the dissociation of py from $VO(acac)_2(py)$.

4. CONCLUSIONS

The nonclassical trimers $(V_3(\mu_3\text{-}O)O_2)(\mu_2\text{-}O_2P(CH_2C_6H_5)_2)_6(H_2O)$, **1**, and $(V_3(\mu_3\text{-}O)O_2)(\mu_2\text{-}O_2P(CH_2C_6H_5)_2)_6(py)$, **2**, can be obtained either under solvothermal reaction conditions or an easier substitution route conducted at room temperature. The presence of absorptions in the IR spectra in the 995 and 1025 cm^{-1} region of intensity 1:2 may signify the nonclassical arrangement. Reactions using diphenylphosphinic acid and 2-hydroxyisophosphindoline-2-oxide resulted in polymeric species. The structural characterization of compounds **1** and **2** was based upon the collection and refinement of data collected from material labeled as crystals **A** and **B**. Crystal **A** consisted entirely of **1** but contained disorder whereby the outer periphery of the ligand structure was maintained but the inner core "$(V_3(\mu_3\text{-}O)O_2)(H_2O)$" was oriented in three different arrangements for **1**. Crystal **B** consisted of a cocrystallization of **1** and **2** in a 21.7(6):78.3(6)% ratio. The structure of pure **2** was also detailed. Different arrangements of the coordinated py ligand were observed. Magnetic susceptibility measurements revealed values close to the spin only value for one unpaired electron for **1**−**5** and this was confirmed by variable temperature magnetic susceptibility and magnetization measurements on complex **2**. Thermal analysis assessed the bond strengths of the ligated water in **1** and the pyridine molecule in **2** at 10.7 and 42.0 kJ/mol respectively, and upon heating to 600 °C the complexes decomposed. Experiments are currently being conducted to see if the aforementioned polymers can be broken into smaller complexes with suitable binding ligands.[48]

■ ASSOCIATED CONTENT

Ⓢ Supporting Information

Table S1 featuring the magnetic data, FTIR spectra of complexes $VO(acac)_2$, $VO(acac)_2(py)$, complexes **1**−**5**, and, crystal **B** Figures S1−S8. X-ray powder patterns for complexes **3**-**5**, Figure S9. TGA plots on $(VO(O_2PPh_2)_2)_\infty$ (**3**), $VO(acac)_2$ and $VO(acac)_2(py)$, Figures S10, S11 and S12, and DSC thermogram of $VO(acac)_2(py)$, Figure S13. TGA on diphenylphosphinic acid, complexes **1** and **2**, Figures S14−S16; FTIR spectrum of the residue from **1**, Figure S17; DSC thermograms of **1** and **2**, Figures S18−S19. This material is also available free of charge via the Internet at http://pubs.acs.org. CCDC's 827865, 827866, and 842909 contain the supplementary crystallographic data for complexes **A**, **B** and **2** respectively. These data can be obtained free of charge from The Cambridge Crystallographic Data Centre via www.ccdc.cam.ac.uk/data_request/cif.

■ AUTHOR INFORMATION

Corresponding Author

*Tel.: 906 487 2309. E-mail: rluck@mtu.edu.

Notes

The authors declare no competing financial interest.

■ ACKNOWLEDGMENTS

The diffractometer used to collect structural data was funded by NSF Grant 0087210, by Ohio Board of Regents Grant CAP-491, and by YSU. Helpful comments from reviewers and Professor L. K. Thompson of Memorial University, Newfoundland, Canada and support by Michigan Technological University is acknowledged.

■ REFERENCES

(1) Feng, L.; Luck, R. L.; Maass, J. S. Syntheses, properties and olefin epoxidation reactivities of "Mo-4O8" clusters stabilized by phosphinate ligands. *Proceedings of the 239th ACS National Meeting*; American Chemical Society: Washington, DC, 2010; p INOR-910.
(2) Jimtaisong, A.; Feng, L.; Sreehari, S.; Bayse, C. A.; Luck, R. L. J. *Cluster Sci.* **2008**, *19*, 181−195.
(3) Jimtaisong, A.; Luck, R. L. J. *Cluster Sci.* **2005**, *16*, 167−184.
(4) Maass, J. S.; Chen, Z.; Zeller, M.; Luck, R. L. *Dalton Trans.* **2011**, *40* (43), 11356−11358.
(5) Herron, N.; Thorn, D. L.; Harlow, R. L.; Coulston, G. W. *J. Am. Chem. Soc.* **1997**, *119*, 7149−7150.
(6) Butler, A.; Sandy, M. *Nature (London, U. K.)* **2009**, *460*, 848−854.
(7) Willsky, G. R.; Goldfine, A. B.; Kostyniak, P. J.; McNeill, J. H.; Yang, L. Q.; Khan, H. R.; Crans, D. C. *J. Inorg. Biochem.* **2001**, *85*, 33−42.
(8) Khan, M. I.; Zubieta, J. *Prog. Inorg. Chem.* **1995**, *43*, 1−149.
(9) Dean, N. S.; Bond, M. R.; O'Connor, C. J.; Carrano, C. J. *Inorg. Chem.* **1996**, *35*, 7643−7648.
(10) Kawasaki, S.; Koikawa, M.; Tokii, T. *Mol. Cryst. Liq. Cryst. Sci. Technol., Sect. A* **2002**, *376*, 365−370.
(11) Koga, K.; Ueno, M.; Koikawa, M.; Tokii, T. *Inorg. Chem. Commun.* **2003**, *6*, 374−376.
(12) Costantino, F.; Midollini, S.; Orlandini, A.; Sorace, L. *Inorg. Chem. Commun.* **2006**, *9*, 591−594.
(13) Norman, R. E.; Holz, R. C.; Menage, S.; Que, L. Jr.; Zhang, J. H.; O'Connor, C. J. *Inorg. Chem.* **1990**, *29*, 4629−37.
(14) Turowski, P. N.; Armstrong, W. H.; Roth, M. E.; Lippard, S. J. *J. Am. Chem. Soc.* **1990**, *112*, 681−90.
(15) Liu, S.-J.; Staples, R. J.; Fackler, J. P. *Polyhedron* **1992**, *11*, 2427−2430.
(16) Cotton, F. A.; Extine, M. W.; Falvello, L. R.; Lewis, D. B.; Lewis, G. E.; Murillo, C. A.; Schwotzer, W.; Tomas, M.; Troup, J. M. *Inorg. Chem.* **1986**, *25*, 3505−12.
(17) Castro, S. L.; Streib, W. E.; Sun, J.-S.; Christou, G. *Inorg. Chem.* **1996**, *35*, 4462−4468.
(18) Chaudhuri, P.; Hess, M.; Weyhermüller, T.; Bill, E.; Haupt, H.-J.; Flörke, U. *Inorg. Chem. Commun.* **1998**, *1*, 39−42.
(19) Cotton, F. A.; Lewis, G. E.; Mott, G. N. *Inorg. Chem.* **1982**, *21*, 3127−30.
(20) Kickelbick, G.; Holzinger, D.; Brick, C.; Trimmel, G.; Moons, E. *Chem. Mater.* **2002**, *14*, 4382−4389.
(21) Boyd, E. A.; Boyd, M. E. K.; Kerrigan, F. *Tetrahedron Lett.* **1996**, *37*, 5425−5426.
(22) Venezky, D. L.; Poranski, C. F. Jr. *J. Org. Chem.* **1967**, *32*, 838−40.
(23) Rowe, R. A.; Jones, M. M. *Inorg. Synth.* **1957**, *5*, 113−116.
(24) Jones, M. M. *J. Am. Chem. Soc.* **1954**, *76*, 5995−5997.
(25) *Bruker Apex2*, version 2.1-4, Bruker AXS Inc.: Madison, WI, U.S.A., 2007.
(26) Sheldrick, G. *Acta Crystallogr.* **2008**, *A64*, 112−122.
(27) Spek, A. L. *Acta Crystallogr.* **2009**, *D65*, 148−155.
(28) Pitts, J. J.; Robinson, M. A.; Trotz, S. I. *J. Inorg. Nucl. Chem.* **1969**, *31*, 3685−90.
(29) La, G. A.; Marucci, G.; Monaci, A. *Gazz. Chim. Ital.* **1964**, *94*, 1459−63.
(30) Podall, H. E.; Iapalucci, T. L. *J. Polym. Sci., Part B: Polym. Lett.* **1963**, *1*, 457−9.
(31) Rosca, I. *Bul. Inst. Politeh. Iasi* **1970**, *16*, 15−24.
(32) Farrugia, L. J. *J. Appl. Crystallogr.* **1997**, *30*, 565.
(33) Macrae, C. F.; Bruno, I. J.; Chisholm, J. A.; Edgington, P. R.; McCabe, P.; Pidcock, E.; Rodriguez-Monge, L.; Taylor, R.; van de Streek, J.; Wood, P. A. *J. Appl. Crystallogr.* **2008**, *41*, 466−470.
(34) Allen, F. H. *Acta Crystallogr.* **2002**, *B58*, 380−388.
(35) Kurotobi, K.; Murata, Y. *Science* **2011**, *333*, 613−616.
(36) Aleksandrov, G. G.; Sergienko, V. S.; Afonin, E. G. *Crystallogr. Rep.* **2001**, *46*, 46−50.
(37) Rocha, J.; Almeida Paz, F. A.; Shi, F.-N.; Ferreira, R. A. S.; Trindade, T.; Carlos, L. D. *Eur. J. Inorg. Chem.* **2009**, *2009*, 4931−4945.
(38) Borras-Almenar, J. J.; Clemente-Juan, J. M.; Coronado, E.; Tsukerblat, B. S. *J. Comput. Chem.* **2001**, *22*, 985−991.
(39) Wieghardt, K.; Bossek, U.; Volckmar, K.; Swiridoff, W.; Weiss, J. *Inorg. Chem.* **1984**, *23*, 1387−9.
(40) Do, J.; Zheng, L.-M.; Bontchev, R. P.; Jacobson, A. J. *Solid State Sci.* **2000**, *2*, 343−351.
(41) Ahmed, M. A. K.; Fjellvåg, H.; Kjekshus, A.; Klewe, B. Z. *Anorg. Allg. Chem.* **2004**, *630*, 2311−2318.
(42) Le Bail, A.; Marcos, M. D.; Amoros, P. *Inorg. Chem.* **1994**, *33*, 2607−2613.
(43) Bircsak, Z.; Hall, A. K.; Harrison, W. T. A. *J. Solid State Chem.* **1999**, *142*, 168−173.
(44) Shibutani, Y.; Shinra, K. *Bull. Chem. Soc. Jpn.* **1989**, *62*, 1477−81.
(45) Dilli, S.; Patsalides, E. *Aust. J. Chem.* **1976**, *29*, 2369−79.
(46) Van Der Voort, P.; White, M. G.; Vansant, E. F. *Langmuir* **1998**, *14*, 106−112.
(47) Satsuma, A.; Hattori, A.; Furuta, A.; Miyamoto, A.; Hattori, T.; Murakami, Y. *J. Phys. Chem.* **1988**, *92*, 2275−2282.
(48) Siqueira, M. R.; Tonetto, T. C.; Rizzatti, M. R.; Lang, E. S.; Ellena, J.; Burrow, R. A. *Inorg. Chem. Commun.* **2006**, *9*, 537−540.